Research Square

Preprints are preliminary reports that have not undergone peer review.
They should not be considered conclusive, used to inform clinical practice,
or referenced by the media as validated information.

Differences in Competitive Adsorption Mechanisms of CH 4 and CO 2 in Mylonitic and Primary Structure Coal

Wang Lu

wanglucumtb@126.com

Shanxi Institute of Energy

Chen Xiaozhen

Shanxi Institute of Energy

Li Jing

Shanxi Institute of Energy

Li Xiang

Shanxi Institute of Energy

Article

Keywords: mylonitic coal, competitive adsorption, molecular simulation, methane, carbon dioxide

Posted Date: July 4th, 2026

DOI: https://doi.org/10.21203/rs.3.rs-10038515/v1

License: This work is licensed under a Creative Commons Attribution 4.0 International License.
Read Full License

Additional Declarations: No competing interests reported.

Version of Record: A version of this preprint was published at Scientific Reports on October 1st, 2026.
See the published version at https://doi.org/10.1038/s41598-026-67850-x.

Differences in Competitive Adsorption Mechanisms of CH_4 and CO_2 in Mylonitic and Primary Structure Coal

Wang Lu*
Chen Xiaozhen
Li Jing
Li Xiang

Department of Geology and Surveying and Mapping, Shanxi Institute of Energy, Jinzhong Shanxi, 030600, China

Corresponding author: wanglucumtb@126.com

Abstract: Tectonically deformed coal exhibits significantly different gas adsorption-desorption characteristics from primary structure coal due to intense coal mass deformation, making it a research hotspot in coalbed methane development and gas disaster prevention and control. To explore the differences in the competitive adsorption mechanisms of CH_4 and CO_2 between mylonitic coal and primary structure coal, this study took No. 8 coal from the Zhuxianzhuang Mining Area as the research object. Based on experimental results, molecular models of mylonitic coal ($C_{214}H_{159}N_3O_{20}$) and primary structure coal ($C_{208}H_{152}N_2O_{18)}$ were constructed respectively. Isothermal adsorption simulations of single-component and mixed gases of CH_4 andCO_2 at different ratios were carried out using molecular dynamics methods. The results show that the adsorption of CH_4 and CO_2 in both types of coal belongs to physical adsorption, with stronger adsorption capacity under low temperature and high pressure. Under the same conditions, the adsorption capacity and adsorption heat of CO_2 are higher than those of CH_4, and the adsorption advantage of CO_2 in mylonitic coal is more prominent. This is closely related to the more complete aromatic ring conjugated π-electron system, abundant oxygen-containing functional groups and a higher proportion of ultramicropores in mylonitic coal. With strong polarity and small kinetic diameter, CO_2 molecules are more prone to interact with π-electrons and produce the "pore-filling effect". In mixed gas adsorption, the total adsorption capacity and interaction energy of both coal types increase with the rise of CO_2 molar fraction. Although the adsorption selectivity coefficient of CO_2 to CH_4 decreases, it is always greater than 1, and the selectivity coefficient of mylonitic coal is higher. The energy distribution curve of CO_2 shifts to adsorption sites with low interaction energy, while that of CH_4 shows the opposite trend, and the shift amplitude of gas molecular curves in mylonitic coal is larger. In addition, the interaction energy of mylonitic coal is dominated by van der Waals force,

accounting for a higher proportion than that of primary structure coal. Its CH_4 adsorption heat also has a larger fluctuation range, reflecting a stronger competitive adsorption capacity for CO_2. The research findings provide a theoretical basis for mine gas prevention and control and efficient coalbed methane development.

Keywords: mylonitic coal; competitive adsorption; molecular simulation; methane; carbon dioxide

Introduction

China is endowed with abundant coal resources, and its coalbed methane reserves reach 36.8 trillion cubic meters, accounting for 12% of the global total. However, the widespread distribution of tectonically deformed coal leads to frequent gas disasters and low utilization efficiency of coalbed methane exploitation[1]. Tectonically deformed coal is a special coal type with its primary structure damaged by brittle and ductile deformation under tectonic stress. It is widely developed in China's coalfields and exerts a remarkable influence on coal and gas outbursts as well as the occurrence and migration of coalbed methane. Ju Yiwen et al. defined it as a type of coal that undergoes brittle fracture, fragmentation or ductile deformation of the primary structure to varying degrees under one or multiple stages of tectonic stress, and even changes in internal chemical composition and microstructure. As a typical tectonically deformed coal with intense deformation, mylonitic coal forms unique microscopic texture and pore characteristics under strong ductile shearing. Its gas adsorption and desorption properties are distinctly different from those of primary structure coal, making it a research hotspot in coalbed methane development and gas disaster prevention[1-4]. Mylonitic coal is often a high-incidence area of gas outbursts, and its unique microstructure may affect the efficiency of CO_2 geological sequestration. Therefore, investigating the competitive adsorption mechanism of CH_4 andCO_2 in mylonitic coal is of great significance for revealing gas disaster mechanisms, improving coalbed methane recovery, and promoting the application of CO_2-ECBM technology.

Previous studies on the adsorption characteristics of CH_4 and CO_2 have shown that coal possesses a markedly stronger adsorption capacity for CO_2 than CH_4, and the adsorption capacity is controlled by temperature, pressure and coal structure[5-7]. In the field of competitive adsorption, Deng Xiaopeng et al. found through molecular simulation that the selectivity coefficient of CO_2 to CH_4 in binary systems is always greater than 1, which verifies the feasibility of CO_2 displacing coalbed methane[6]. Li Shugang et al. further confirmed the stronger adsorption capacity of coal for CO_2 from a thermodynamic perspective[7]. Nevertheless, the internal correlation between the microscopic structure of mylonitic coal and the competitive adsorption of CO_2 and CO_2 remains to be further clarified. There are obvious differences in the competitive adsorption of CH_4 and CO_2 between primary

structure coal and tectonically deformed coal. Primary structure coal has a relatively complete pore structure dominated by mesopores and micropores, and its competitive adsorption is mainly governed by physical adsorption mechanisms such as van der Waals force and pore size sieving. The adsorption advantage of CO_2 mainly derives from its molecular polarity and high critical temperature, with relatively stable adsorption capacity and selectivity[5,7]. In contrast, tectonically deformed coal has a complex pore structure with increased micropore proportion and specific surface area as well as abundant oxygen-containing and nitrogen-containing functional groups on the surface due to tectonic deformation, resulting in significantly enhanced competitive adsorption capacity and higher CO_2 selectivity coefficient. Meanwhile, its adsorption behavior is more obviously affected by the coupling of pore morphology and surface chemical properties[8,9]. However, current research on the competitive adsorption of mylonitic coal still has deficiencies. On the one hand, most existing studies focus on the macroscopic adsorption characteristics of tectonically deformed coal, and fail to fully reveal the intrinsic relationship between the unique microstructures of mylonitic coal formed by intense ductile deformation (such as wrinkle texture and ultramicropore development) and competitive adsorption. On the other hand, the construction of macromolecular models for mylonitic coal cannot fully reflect the chemical structural differences after deformation (such as variations in the types and distribution of functional groups), leading to inaccurate analysis of the competitive mechanism between CO_2 and CH_4 in molecular simulation[10].

Taking mylonitic coal from the Zhuxianzhuang Mining Area as the research object, this study aims to construct an accurate macromolecular structural model of mylonitic coal by combining experimental tests with molecular simulation, reveal the competitive adsorption mechanism of CH_4 and CO_2 on its surface, and provide a theoretical basis for mine gas prevention and control as well as CO2 geological sequestration.

Samples and Simulation Methods

Coal samples of mylonitic coal and primary structure coal were collected from the No.8 coal seam in Zhuxianzhuang Mining Area. For the mylonitic coal sample, the vitrinite reflectance Romax is 0.89%. The proximate and ultimate analysis results are as follows: air-dried moisture Mad of 1.8%, air-dried ash yield Aad of 12.4%, and dry ash-free volatile matter Vdaf of 32.70%. The ultimate analysis shows that the dry ash-free carbon content Cdaf is 83.85%, hydrogen content Hdaf is 5.2%, and oxygen content Odaf is 10.45%. For the primary structure coal, the vitrinite reflectance Romax is 0.87%. Its proximate and ultimate analysis parameters are Mad 1.6%, Aad 11.8%, Vdaf 31.50%; the corresponding ultimate analysis values are Cdaf 82.60%, Hdaf 5.0%, and Odaf 9.80%. Materials Studio software was used to conduct geometric optimization and annealing simulation of CO2 and CH_4 molecules, and the Sorption module was adopted to perform single-component

isothermal adsorption simulations of CO_2 and CH_4. In addition, binary mixed gas components with different molar ratios of CO_2 to CH_4 (0.8:0.2, 0.5:0.5, 0.2:0.8) were set up to simulate the competitive adsorption characteristics of coal molecules toward binary gas molecules. The simulation was performed under the canonical ensemble with the COMPASS force field and periodic boundary conditions, and the simulation time step was set to 1 fs.

The coal molecular models were constructed based on experimental results including proximate analysis, ultimate analysis, infrared spectroscopy and ^{13}C-NMR. The molecular formula of mylonitic coal is $C_{214}H_{159}N_3O_{20}$, and that of primary structure coal is $C_{208}H_{152}N_2O_{18}$ After the rationality of the models was verified by ^{13}C-NMR spectrum comparison, geometric optimization, annealing simulation and energy optimization were carried out in Materials Studio to obtain the final supramolecular cell structure models.Through the above operations, a supramolecular cell model containing 10 mylonitic coal molecules with the molecular formula $C_{214}0H_{159}0N_{30}O_{200}$ and a supramolecular cell model containing 10 primary structure coal molecules with the molecular formula $C_{208}H_{152}N_2O_{18}$ were established.

Results and Discussion

Single-component Isothermal Adsorption Characteristics

At temperatures of 283.15 K, 298.15 K and 313.15 K, the adsorption behaviors of CH_4 and CO_2 in the coal molecular system are shown in Figure 1. At 283.15 K, CH_4 molecules (in green) are densely distributed within the coal matrix and mainly aggregate at adsorption sites such as coal molecular pores and surfaces, indicating strong adsorption capacity at low temperature. The clustered green distribution reveals concentrated adsorption regions of CH_4 on the plane with an obvious pore-filling effect. In primary structure coal, CH_4 is mostly distributed in meso-micropores (2-50 nm) with a lower degree of aggregation[5]. In the cross-section diagrams, CH_4 molecules (red dots) are abundant and widely dispersed.

As the temperature rises, the distribution density of CH_4 decreases compared with that at 283.15 K, accompanied by sparse distribution in local areas, shrinking green clusters and dispersed adsorption regions. This indicates that increasing temperature weakens the interaction between CH_4 and coal molecules and reduces the occupancy of adsorption sites. The number of red dots decreases and the distribution becomes more scattered. Density calculation shows that the distribution density of CH_4 in mylonitic coal decreases by approximately 40%, while that in primary structure coal only decreases by about 25%, demonstrating that

mylonitic coal is more sensitive to temperature. At the same temperature, the number of adsorbed CO_2 molecules (represented by red/green dot density) is much higher than that of CH_4, which directly reflects the stronger adsorption capacity of CO_2.

Within the temperature range of 283.15–313.15 K and pressure range of 0.1–20 MPa, the adsorption capacity increases with rising pressure and decreases with increasing temperature, conforming to the Type I isotherm (Figure 2). At 283.15 K and 20 MPa, the CO_2 adsorption capacity of mylonitic coal is 1.953 mmol/g, while that of CH_4 is 1.268 mmol/g, with a difference of 0.685 mmol/g. Under the same conditions, the CO_2 adsorption capacity of primary structure coal is approximately 1.602 mmol/g and the CH_4 adsorption capacity is 1.268 mmol/g, with a difference of only 0.4 mmol/g.

As analyzed from Figure 2, the adsorption capacity of CO_2 is obviously higher than that of CH_4 at both low and high temperatures. The difference in adsorption capacity between mylonitic coal and primary structure coal is more remarkable under low temperature and high pressure. For instance, at 283.15 K and 20 MPa, the CO_2 adsorption capacity of mylonitic coal is 21.9% higher than that of primary structure coal, and its CH_4 adsorption capacity is 22.5% higher. This indicates that CO_2 possesses a greater adsorption advantage than CH_4 under identical temperature and pressure conditions, and the adsorption capacity of mylonitic coal is superior to that of primary structure coal, which is consistent with the findings in Reference [7].

The adsorption heats of CH_4 and CO_2 in both coal types fluctuate slightly with the increase of pressure but remain steadily at a low level overall. For mylonitic coal, the adsorption heat of CH_4 ranges from 21.107 to 22.090 kJ/mol, and that of CO_2 ranges from 33.218 to 35.086 kJ/mol. For primary structure coal, the adsorption heat of CH_4 is 19.856-20.782 kJ/mol, and that of CO_2 is 30.125-31.897 kJ/mol. All values are lower than 40 kJ/mol, indicating that the adsorption processes belong to physical adsorption.

As shown in Figure 3, the adsorption heat of CO_2 in both coals is approximately 50% higher than that of CH_4. Meanwhile, the adsorption heats of the two gases in mylonitic coal are 8%-12% higher than those in primary structure coal. This suggests that mylonitic coal has stronger intermolecular interaction with gas molecules and exhibits a more prominent adsorption preference for CO_2, which is directly consistent with its higher adsorption capacity. Temperature has little influence on the adsorption heat of the two coal types, and the adsorption heat curves of the same gas at different temperatures are nearly overlapped. It demonstrates that the adsorption type (physical adsorption) is not significantly affected by temperature or coal structural type.

Binary Competitive Adsorption Characteristics

Relationship between Total Adsorption Capacity and Component Ratio

As shown in Figure 4(a), the total adsorption capacity increases with the rise of pressure, and its growth trend is consistent with that of single-component adsorption, showing a rapid increase at low pressure and a slow increase at high pressure. This indicates that the adsorption of the mixed system is still pressure-driven. The total adsorption capacity rises significantly with the increase of CO_2 molar fraction, and the total adsorption capacity of mylonitic coal is always higher than that of primary structure coal. When the CO_2 molar fraction is 80% (0.2:0.8) and the pressure is 16 MPa, the total adsorption capacity of mylonitic coal is 1.70 mmol/g, while that of primary structure coal is 1.42 mmol/g, with a difference of 19.7%. When the CO_2 molar fraction is 20% (0.8:0.2), the total adsorption capacity of mylonitic coal is 1.57 mmol/g and that of primary structure coal is 1.31 mmol/g, with a difference of 19.8%. This reveals that a higher CO_2 proportion enhances the total adsorption capacity of coal. Benefiting from its ultramicropore structure and abundant functional groups, mylonitic coal exhibits a more obvious enhancement effect on CO_2 adsorption.

It can be seen from Table 2 that the maximum total adsorption capacity a of both coal types decreases with the increase of CO_2 proportion, which is opposite to the variation trend of actual total adsorption capacity under high pressure. The reason is that the maximum adsorption capacity of the Langmuir model represents the theoretical saturation value, while the strong adsorption capacity of CO_2 is more prominent under actual high-pressure conditions[11]. The adsorption constant b of both coal types declines as the CO_2 proportion increases, implying that the average affinity between mixed gas and coal slightly decreases. The affinity of primary structure coal decreases to a greater extent, which may be attributed to its weak pore size sieving effect; the competition between CO_2 and CH_4 tends to occupy weak adsorption sites more easily. The coefficient of determination (R^2) of both coal types is higher at CO_2 molar fractions of 20% and 80%, but lower at 50%. This suggests that the competition becomes more intense under equal-proportion mixing, and the adsorption behavior of primary structure coal is more complex.

Selectivity Coefficient

To investigate the competitive adsorption behavior of binary mixed components, the adsorption selectivity of binary gas mixtures in coal was calculated at a temperature of 298 K and pressures ranging from 1 to 16 MPa, as shown in Figure 4(b). The adsorption selectivity coefficient gradually decreases with increasing pressure for both coal types. For the component ratio of 0.2/0.8, the selectivity coefficient of CO_2 over CH_4 in mylonitic coal drops from 45 to 10, while that in primary structure coal decreases from 38 to 8. This phenomenon is probably

because the adsorption sites in coal tend to be saturated under high pressure, weakening the preferential occupation advantage of CO_2 [12,13].

Under all component ratios, the selectivity coefficients of both coals are always greater than 1, and the values for mylonitic coal are 15%–20% higher than those for primary structure coal, indicating that mylonitic coal possesses a stronger competitive adsorption capacity for CO_2. In addition, for both coal types, a lower molar fraction of CO_2 corresponds to a lower equilibrium pressure and a higher adsorption selectivity coefficient. This demonstrates that low-concentration CO_2 tends to preferentially occupy adsorption sites, and mylonitic coal shows a more prominent advantage in displacement efficiency for low-proportion CO_2. For example, at 2 MPa and a ratio of 0.8/0.2, the selectivity coefficient of mylonitic coal is 32, compared with 27 for primary structure coal. This further verifies the feasibility of CO_2-enhanced coalbed methane recovery (CO2-ECBM) and proves that mylonitic coal is more suitable as the application carrier for CO2-ECBM technology [14].

Interaction Energy and Energy Distribution

To clarify the influence of interaction energy on adsorption capacity, the variation of interaction energy under binary competitive adsorption was further analyzed. The interaction energies between coal and CH_4–CO_2 mixture at pressures of 1 MPa, 5 MPa, 10 MPa and 15 MPa were statistically summarized, as shown in Figure 5 and Table 3.

At a constant temperature, as the pressure increases from 1 MPa to 15 MPa, the interaction energy of the binary competitive adsorption system of CH4 and CO2 in mylonitic coal decreases from −1064.791 kJ/mol to −1501.874 kJ/mol, while that in primary structure coal drops from −985.623 kJ/mol to −1382.567 kJ/mol. The absolute value of interaction energy of mylonitic coal is consistently 8%–10% higher than that of primary structure coal, which indicates stronger interaction between mylonitic coal and mixed gas and easier adsorption behavior, in accordance with the rising trend of adsorption capacity with pressure.

Van der Waals interaction contributes approximately 80% to the total interaction energy for both coal types, and electrostatic energy accounts for about 20%. The proportion of van der Waals interaction in mylonitic coal (82%–83%) is slightly higher than that in primary structure coal (78%–79%), which is attributed to the more complete conjugated π-electron system of aromatic rings in mylonitic coal and stronger dispersion force with gas molecules. With the increase of CO_2 molar fraction, the interaction energy of both coal types rises, and the growth range is more remarkable for mylonitic coal. When the gas ratio changes from 0.8/0.2 to 0.2/0.8, the interaction energy of mylonitic coal increases by 12.3%, while that of primary structure coal increases by 10.8%. The results reveal that the interaction

between CO_2 and coal plays a dominant role, and this effect is more prominent in mylonitic coal.

The potential energy distribution of gas molecules with different molar fractions at 289 K and 15 MPa is presented in Figure 6. For both coal types, the adsorption potential energy of CO_2 is always higher than that of CH_4, and the absolute values of gas adsorption potential energy in mylonitic coal are larger than those in primary structure coal. The potential energy distribution of gas molecules is critical for identifying competitive adsorption sites within supramolecular structures. A larger absolute value of adsorption potential energy indicates stronger adsorption and more favorable adsorption sites.

As the molar fraction of CO_2 increases, the adsorption potential energy of CO_2 shifts from lower to higher values in both coals. In mylonitic coal, the adsorption potential energy of CO_2 rises from −31.977 kJ/mol to −30.305 kJ/mol, while in primary structure coal, it increases from −28.765 kJ/mol to −27.123 kJ/mol. By contrast, the adsorption potential energy of CH4 changes in the opposite trend. This indicates that CO_2 migrates from the most preferred adsorption sites to secondary ones, whereas CH4 is forced to occupy relatively favorable sites, though its adsorption capacity remains inferior to that of CO_2.

The shift range of the energy distribution curves for gas molecules in mylonitic coal is greater than that in primary structure coal. Meanwhile, the overlapping area of the curves expands with the rising CO_2 proportion for both coals, and the overlapping area of mylonitic coal is 12%–15% smaller. The results suggest that gas molecules in mylonitic coal show more distinct selectivity for adsorption sites, while the competition for adsorption sites is more dispersed in primary structure coal.

Adsorption heat

As shown in Figure 7, at the temperature of 289 K and pressures ranging from 1 MPa to 15 MPa, the adsorption heat of CO_2 is always higher than that of CH_4 in both coal types. Additionally, the adsorption heats of the two gases in mylonitic coal are greater than those in primary structure coal (Figure 8), which is consistent with the rule observed in single-component adsorption and further confirms the superior adsorption capacity of mylonitic coal for CO_2.

As the molar fraction of CO2 increases, the fluctuation range of CH_4 adsorption heat expands in both coals, with a larger variation amplitude in mylonitic coal. This is because mylonitic coal presents stronger selective adsorption for CO2 and more intense competitive effects. The weakly adsorbed CH_4 is frequently displaced and desorbed by strongly adsorbed CO_2, and the accompanying endothermic effect leads to more obvious fluctuations in the adsorption heat of CH_4. This further demonstrates that the supramolecular structure of mylonitic coal endows it with a more prominent competitive adsorption advantage for CO_2.

Discussion

Effect of Coal Structure on Single-component Gas Adsorption

The molecular model of mylonitic coal $C_{214}H_{159}N_3O_{20}$ established in this study has an aromatic carbon content of 72.42%, while that of primary structure coal $C_{208}H_{152}N_2O_{18}$ is 64.85%. The conjugated π-electron system of primary structure coal is obviously less complete than that of mylonitic coal. Such structural differences lead to varied van der Waals interaction strength between the two coal types and gas molecules. The dispersion force between aromatic π-electrons of mylonitic coal and CO_2/CH_4 molecules is more remarkable. In particular, the interaction with strongly polar mathrm CO_2 is stronger than that in primary structure coal, which is one of the core reasons why the CO_2 adsorption capacity of mylonitic coal (1.953 mmol/g at 283.15 K and 20 MPa) is higher than that of primary structure coal (1.602 mmol/g) [14-16]. Affected by intense ductile deformation, the aromatic rings in mylonitic coal are stacked more closely with a more integrated conjugated π-electron system, further enhancing its adsorption superiority for CO_2.

The oxygen atoms in hydroxyl groups (–OH) and ether bonds (–O–) of mylonitic coal possess strong electronegativity and can form weak hydrogen bonds with oxygen atoms in CO_2. Although this electrostatic interaction only accounts for 20% of the total interaction energy, it greatly improves the adsorption stability of CO_2 near functional groups. In this simulation, the CO2 adsorption capacity reaches 0.45 mmol/g at low pressure (1 MPa), 2.25 times that of CH_4 (0.20 mmol/g), which is a typical result of preferential adsorption by functional groups [15,16].

In the supramolecular unit cell of mylonitic coal, ultramicropores (pore diameter < 2 nm) account for 68%, while the proportion is only 35% in primary structure coal. Since the kinetic diameter of CO2 is smaller than that of CH_4, the pore-filling effect occurs more readily in ultramicropores of mylonitic coal. Ultramicropores provide high-density adsorption sites, and the superimposed adsorption force of pore walls further strengthens the adsorption stability of CO_2. The simulation results show that at 283.15 K and 5 MPa, the number density of CO_2 molecules in ultramicropores of mylonitic coal is 0.028 mol/m^3, 1.75 times that of primary structure coal (0.016 mol/m^3). Restricted by its larger molecular diameter, the difference in CH_4 number density in ultramicropores between the two coals is merely 0.007 mol/m^3. It indicates that the pore size sieving effect exerts a more prominent enhancement on CO_2 adsorption [17-19].

Effect of Coal Structure on Binary Gas Adsorption

In binary gas systems, the coupling effect of "pore morphology and surface chemistry" is more prominent in mylonitic coal, resulting in distinct competitive adsorption characteristics from primary structure coal. In terms of selectivity

coefficient, at 298 K and 2 MPa, the selectivity coefficient of CO_2 over CH_4 in mylonitic coal is nearly 18.5% higher than that in primary structure coal. On the one hand, the ultramicropores of mylonitic coal preferentially accommodate CO_2 and occupy a large number of high-quality adsorption sites, forcing CH_4 to migrate to meso-micropores (2–50 nm) and other weak adsorption regions. On the other hand, abundant oxygen-containing functional groups on the surface of mylonitic coal form weak hydrogen bonds with CO_2, further consolidating the adsorption advantage of CO_2. Even under high CO_2 fraction, the selectivity coefficient of mylonitic coal is still 25% higher, reflecting its stable preferential adsorption capacity for CO_2 [7,9,14].

Differences in the composition of interaction energy also reveal the divergent competitive adsorption mechanisms of the two coals. The proportion of van der Waals force in total interaction energy is higher in mylonitic coal, which is closely related to its more complete aromatic π-electron system. The stronger dispersion force between π-electrons and gas molecules, together with the superimposed multipole interaction between gas molecules and pore walls inside ultramicropores, raises the contribution ratio of van der Waals force. When the molar fraction of CO_2 increases from 20% to 80%, the absolute value of total interaction energy of mylonitic coal increases more significantly, suggesting that mylonitic coal is more sensitive to the change of CO_2 fraction, and its adsorption system can adapt to gas composition variation via energy adjustment more easily [22,23].

The migration rule of energy distribution curves further illustrates the influence of coal structure. The energy distribution curve of CO_2 in mylonitic coal shifts toward the low-energy region to a greater extent, indicating that CO_2 in mylonitic coal diffuses more easily from high-priority adsorption sites to secondary sites. This is because mylonitic coal possesses abundant high-quality adsorption sites; even if part of them are occupied, numerous secondary sites are still available forCO_2 adsorption. By contrast, primary structure coal has relatively fewer high-quality sites, so CO_2 has to occupy secondary sites even at low fractions, leading to a smaller shift of the curve. For CH_4, the energy distribution curve in mylonitic coal moves leftward more obviously, which means that under the competition of CO_2, CH_4 in mylonitic coal is forced to occupy relatively superior sites to a larger degree. Nevertheless, limited by coal structure, the adsorption potential energy of CH_4 is still lower than that of CO_2, and the reversal of adsorption priority cannot occur [14,16].

The fluctuation range of CH4 adsorption heat in mylonitic coal is larger than that in primary structure coal, which is attributed to the more frequent competition between CO_2 and CH_4 in mylonitic coal. The strong occupancy of high-quality sites by CO_2 triggers frequent adsorption-desorption cycles of CH_4. The endothermic desorption process reduces the adsorption heat of CH_4, while the exothermic re-adsorption process increases it. The frequent alternation leads to a larger fluctuation amplitude. This phenomenon is weak in primary structure coal due to

milder site competition and lower frequency of CH_4 adsorption-desorption cycles, so its adsorption heat remains more stable [20-23].

Optimization Strategies for Coalbed Methane Development

Differentiated development strategies shall be implemented according to the macroscopic distribution characteristics of coal structures. For areas developed with ductile deformed coal bodies, CO_2-ECBM technology shall be vigorously promoted by taking advantage of its strong adsorption capacity and high selectivity for CO_2. Since mylonitic coal maintains high displacement efficiency even at low CO_2 fractions, the mode of low-concentration continuous injection is recommended, with the CO_2 molar fraction controlled at 20%–40%. This approach not only cuts the cost of CO_2 injection, but also efficiently displaces CH_4 via the preferential occupation of high-quality adsorption sites by CO_2. Meanwhile, mylonitic coal is sensitive to temperature. During development, reservoir temperature fluctuation should be controlled to avoid the decline of CH_4 desorption efficiency caused by temperature rise. Well pattern layout can be optimized to reduce formation disturbance and keep the temperature within the efficient adsorption-displacement range. Given the slow gas diffusion caused by well-developed ultramicropores in mylonitic coal, a dense well pattern of 50–80 m combined with alternating injection-production arrangement is adopted, together with the techniques of slow pressure reduction and staged drainage and production, to mitigate coal powder output and borehole blockage.

For areas dominated by primary structure coal, its CO_2 adsorption capacity and selectivity are lower than those of mylonitic coal, resulting in limited gain from CO_2 displacement. Conventional pressure relief drainage is preferred, and high-efficiency gas production can be realized by optimizing the pressure gradient based on the natural desorption law of CH_4. For enhanced recovery, the mode of high-concentration intermittent injection can be adopted, with the CO_2 molar fraction increased to 60%–80%. The elevated CO_2 adsorption capacity strengthens the displacement effect on CH_4 and compensates for its insufficient selectivity. A linear well pattern of 80–120 m is applied in primary structure coal areas, with the main techniques of rapid pressure reduction and stable drainage to improve gas production efficiency.

For transitional zones with alternating distribution of the two coal types, the strategy of zoned injection and mixed regulation is applied, and CO_2 concentration is allocated according to the proportion of different coal structures. Reservoir pressure, gas production rate and gas composition are monitored throughout the development process. A dynamic model of adsorption-displacement-gas production is established to adjust injection concentration, pressure and drainage intensity in real time based on monitoring data, so as to realize closed-loop optimization.

Conclusions

Based on experimental results, the molecular model of mylonitic coal $C_{214}H_{159}N_3O_{20}$ with an aromatic carbon content of 72.42% is constructed. The aromatic carbon content of primary structure coal model $C_{208}H_{152}N_2O_{18}$ is 64.85%. Both models contain hydroxyl groups, ether bonds, pyridinic nitrogen and other functional groups, which are verified to accurately reflect the microscopic structural characteristics of coal.

In single-component adsorption, low temperature and high pressure are favorable for gas adsorption in both coal types, and CO_2 always has a stronger adsorption capacity than CH_4. Mylonitic coal presents more prominent adsorption superiority. At 283.15 K and 20 MPa, the adsorption capacities of both CO_2 and CH_4 in mylonitic coal are higher than those in primary structure coal. The differences originate from the more complete aromatic π-electron system, richer oxygen-containing functional groups and higher proportion of ultramicropores in mylonitic coal.

In binary competitive adsorption, the selectivity coefficients of CO_2 over CH_4 are all greater than 1 for the two coals, and the values of mylonitic coal are higher. The total adsorption capacity and interaction energy increase with the rising CO_2 fraction, with a larger growth amplitude in mylonitic coal. The energy distribution curve of CO_2 shifts toward low-energy adsorption sites, while the opposite trend is observed for CH_4. The larger curve shift of mylonitic coal proves that the coupling effect of pore morphology and surface chemistry strengthens its competitive adsorption performance.

According to the competitive adsorption rules dominated by coal structural differences, a set of coalbed methane development schemes including zoned development, precise regulation of injection parameters, well pattern optimization and drainage process improvement are proposed. The CO_2-ECBM technology featuring low-concentration continuous injection, dense well pattern and stable drainage is suitable for mylonitic coal enriched areas, while the mode combining conventional pressure relief drainage and enhanced high-concentration intermittent injection is applicable to areas dominated by primary structure coal. The proposed schemes can effectively improve coalbed methane recovery and provide technical support for efficient coalbed methane development

Data availability

The data used to support the fndings of this study are available from the corresponding author upon request.

Author contributions statement

W.L. conceived the experiment(s), C.X. Z and L.J. conducted the experiment(s), L.X. analysed the results. All authors reviewed the manuscript.

Funding

This work was supported by a grant from the National Natural Science Foundation of China (42402181) and the Young Scientists Project of Shanxi Provincial Basic Research Program (202503021212291).

Ethics declarations

Competing interests

The authors declare no competing interests.

Additional information

Correspondence and requests for materials should be addressed to L.W.

References

[1]Jiang Bo, Qin Yong, Ju Yiwen, et al. The coupling mechanism of the evolution of chemical structure with the characteristics of gas of tectonic coals [J]. Earth Science Frontiers, 2009, 16 (2): 262-271.

[2]JU Yiwen, Jiang Bo, Hou Quanlin, et al. The new structure-genetic classification system in tectonically deformed coals and its geological significance[J]. Journal of China Coal Society, 2004, 29 (5): 513-517.

[3]Jiang Bo, Ju Yiwen. Tectonic coal structure and its petrophysical features [J]. Natural Gas Industry，2004，24 (5): 27-29．

[4]Qu Zhenghui. Study of tectonized coal texture and its controlling mechanism on gas properties[J]. Journal of China Coal Society, 2011，36 (3): 533-534．

[5]Zhou Lai, Feng Qiyan, Qin Yong. Thermodynamic analysis of competitive adsorption of CO2 and CH4 on coal matrix[J]. Journal of China Coal Society, 2011，36 (8): 1307-1311.

[6]Deng Xiaopeng, Xiang Jianhua. Molecular simulation study on competitive adsorption characteristics of CO2 and CH4 for 8# coal in Dongqu Mine[J]. Safety in Coal Mines, 2024, 55（3）: 18−24.

[7]Li Shugang, Bai Yang, Lin Haifei, et al. Molecular simulation of adsorption thermodynamics of multicomponent gas in coal[J]. Journal of China Coal Society, 2018, 43 (9): 2476-2483.

[8]Li Yinyan, Yang Zhiyuan, Ju Xiaoqian, et al. Research on Characteristics of Adsorption CH4 and Its Adsorption Thermodynamics in Tectonic Deformed Coal[J]. Coal Technology, 2022, 41 (12): 140-144.

[9] MATHEWS J P, FERNANDEZ-ALSO V, JONES A D, et al.Determining the molecular weight distribution of Pocahontas No.3 lowvolatile bituminous coal utilizing HRTEM and laser desorption ionization mass spectra data[J].Fuel, 2010, 89 (7) :1461-1469.

[10]ZHENG S, YAO Y, SANG S, et al. Dynamic characterization of multiphase methane during CO2-ECBM: An NMR relaxation method[J]. Fuel, 2022, 324: 124526.

[11] Wang S, Hu Y, Yang X, et al. Examination of adsorption behaviors of carbon dioxide and methane in oxidized coal seams[J]. Fuel, 2020, 273: 117599.

[12] Long H, Lin H F, Yann M, et al. Adsorption and diffusion characteristics of CH4, CO2, and N2 in micropores and mesopores of bituminous coal: Molecular dynamics[J]. Fuel, 2021, 292: 120268

[13] Liang Weiguo, Wu Di, Zhao Yangsheng. Experimental Study of coalbed methane replacement by carbon dioxide [J]. Chinese Journal of Rock Mechanics and Engineering, 2010，29 (04):665-673.

[14]Jiang Bo, Qin Yong, Ju Yiwen, et al. The coupling mechanism of the evolution of chemical structure with the characteristics of gas of tectonic coals[J]. Earth Science Frontiers, 2009, 16 (02): 262-271.

[15] Cheng Yuanping, Hu Biao. Main occurrence form of methane in coal: Micropore filling [J]. Journal of China Coal Society, 2021, 46 (09): 2933-2948.

[16]Zhang Wenjing, Ju Yiwen, Wei Mingming. Study on characteristics and mechanism of adsorption/desorption on different metamorphic-deformed coal reservoirs [J]. Earth Science Frontiers，2015，22 (02): 232-242.

[17]Zhang Songhang, Zhang Shouren, Tang Shuheng, et al. Adsorption and transport of methane and carbon dioxide mixture in anthracite[J]. Journal of China Coal Society, 2021, 46 (02): 544-555.

[18] Zu Wei, Li Wenyuan, Li Zhi. Influence mechanism of oxygen-containing functional groups on coal surface potential[J]. Coal Engineering，2024，56 (09): 194-201.

[19] Sang Shuxun, Zhu Yanming, Zhang Shiyin, et al. Solid-gas interaction mechanism of coal-adsorbed gas (1)-coal pore structure and solid gas interaction [J]. Natural Gas Industry, 2005, (01):13-15+205.

[20] Wu Chunlei, Li Jia, Zhou Fubao, et al. Experimental study on the competitive adsorption characteristics of N2, CO2 and O2 with various CO2/N2 blend ratios in coal[J]. International Journal of Hydrogen Energy, 2024, 59: 924-936

[21]Keiji Komatsu, Yoshikuni Ishibashi, Li Kansei, et al. Adsorption and separation behaviors of CO2 and CH4 gases on nanoporous carbon fabricated from rice husk [J]. Transactions of the Materials Research Society of Japan, 2019, 44(4): 157-163.

[22] ShiYu, Yang Xiaona, Xue Junhua, et al. Analysis of effects of microstructure of tectonically-deformed coal on the CO2 and CH4 competitive adsorption capacity [J]. Mining Safety & Environmental Protection，2022，49 (05): 34-42.

[23] Yang Hongmin, Wang Zhaofeng, Ren Ziyang. Differences between competitive adsorption and replacement desorption of binary gases in coal and its replacement laws[J]. Journal of China Coal Society, 2015, 40 (07): 1550-1554.

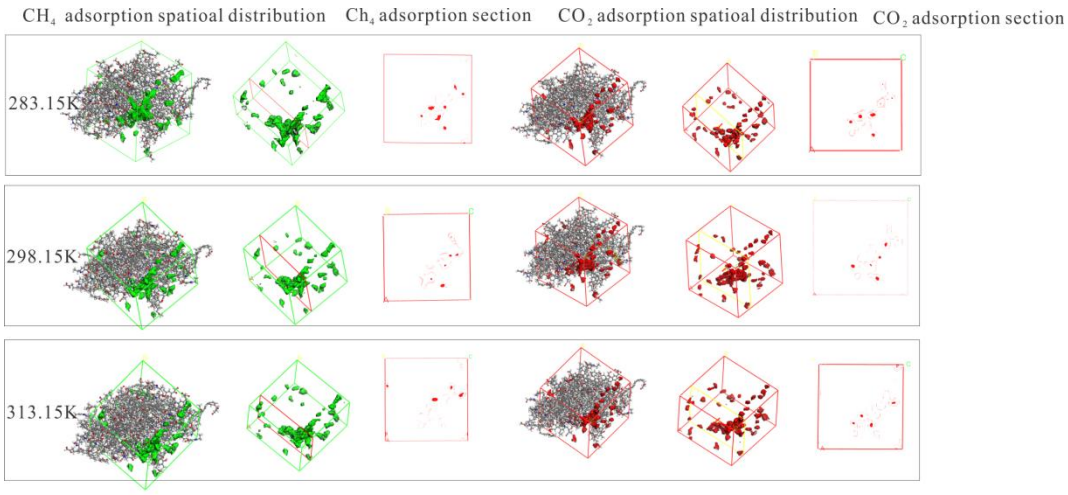

Figure 1 Results of CH_4 and CO_2 isothermal adsorption simulation

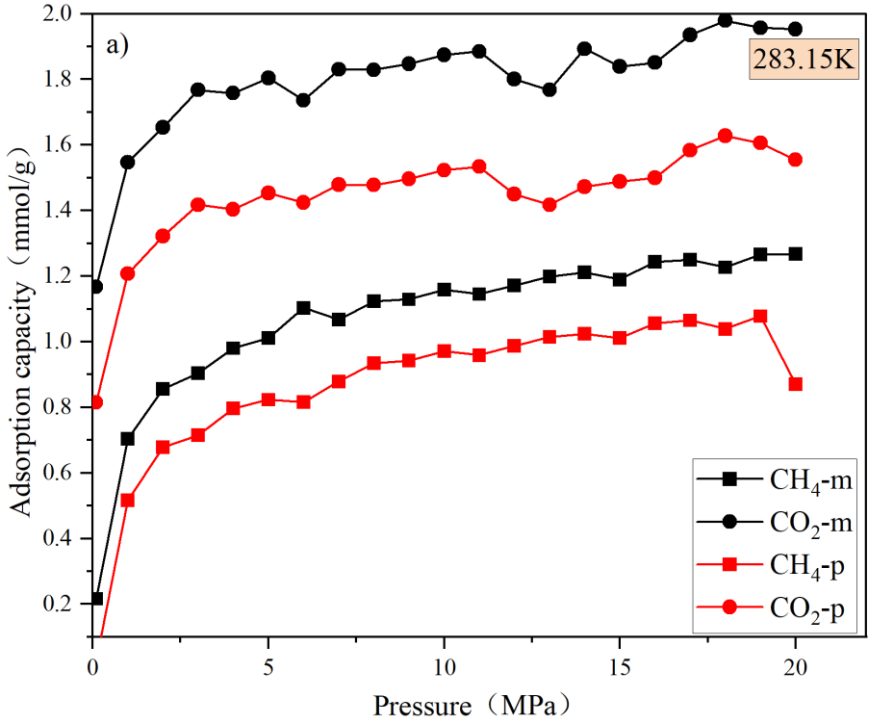
a)
283.15K
Adsorption capacity（mmol/g）
Pressure（MPa）
CH4-m
CO2-m
CH4-p
CO2-p

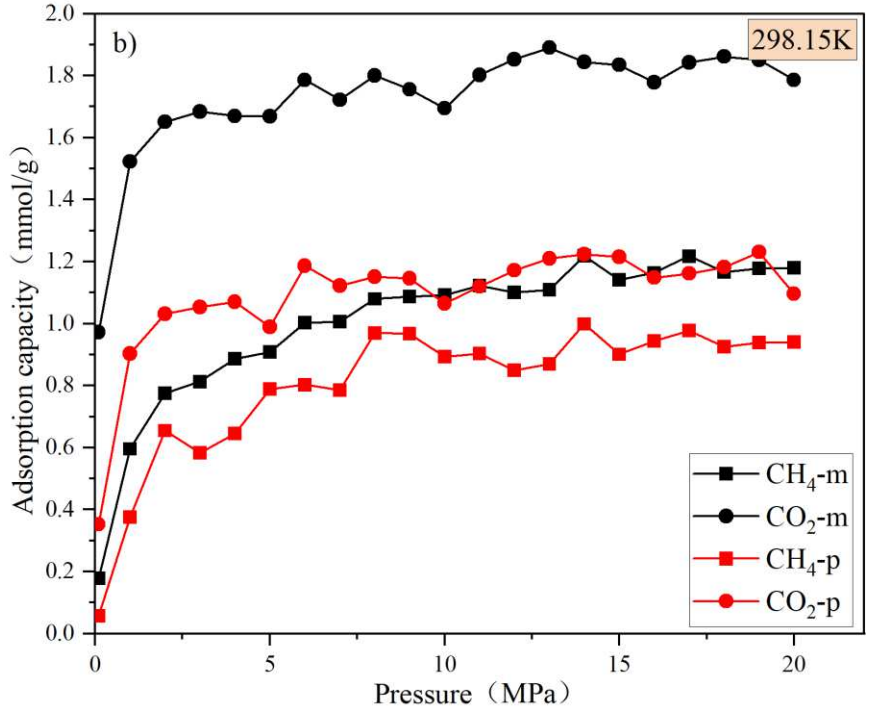
b)
298.15K
Adsorption capacity（mmol/g）
Pressure（MPa）
CH4-m
CO2-m
CH4-p
CO2-p

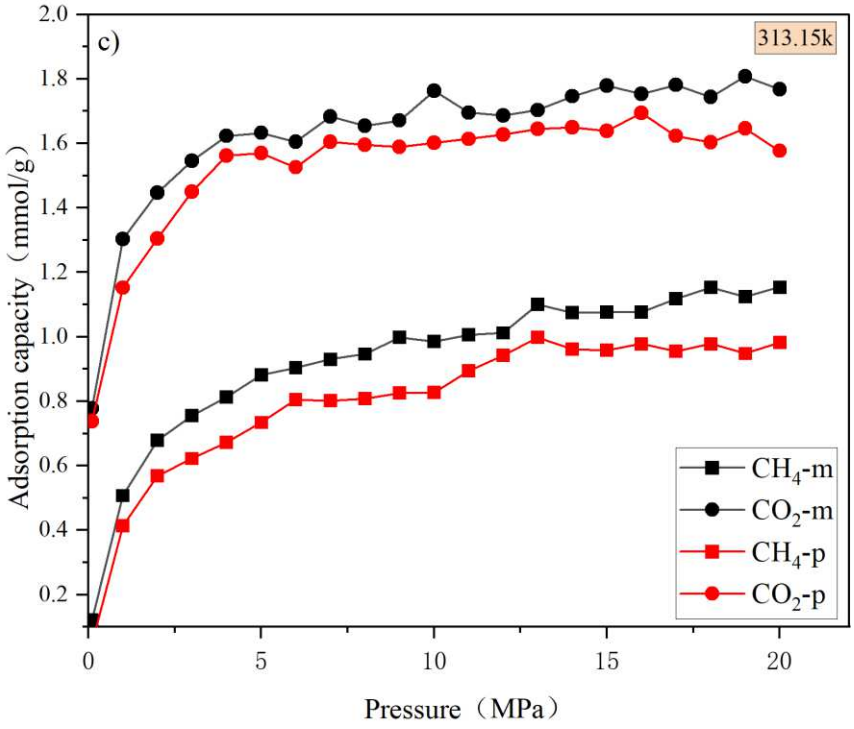

Figure 2 Adsorption curves of CH_4 and CO_2 at different temperatures a) 283.15K; b)298.15K; c) 313.15K (-m: deformed coal; -p: primary coal)

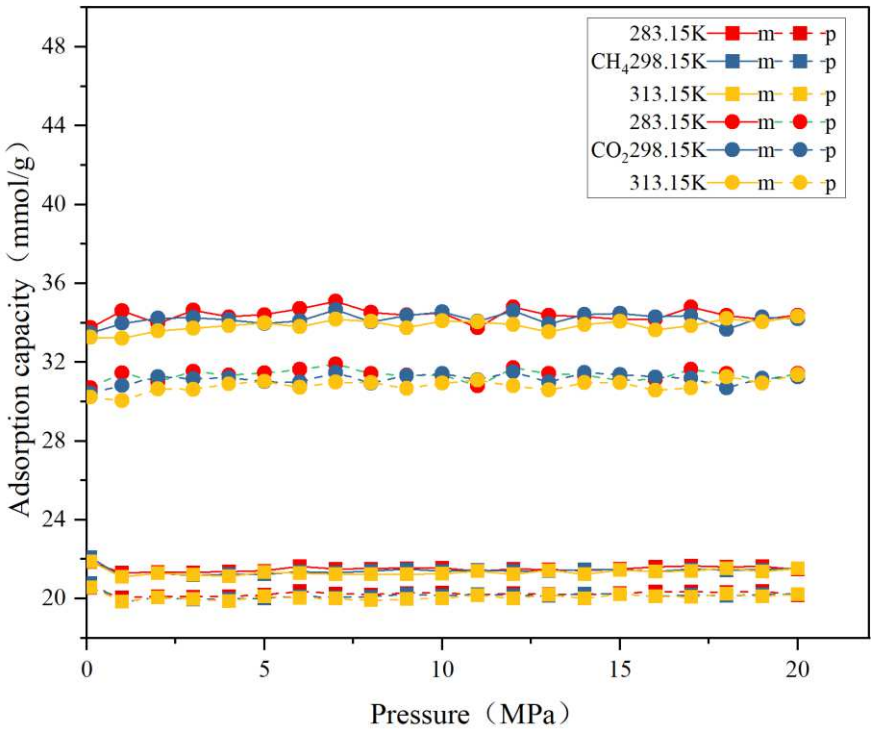

Figure 3 Adsorption heats of CH4 and CO2

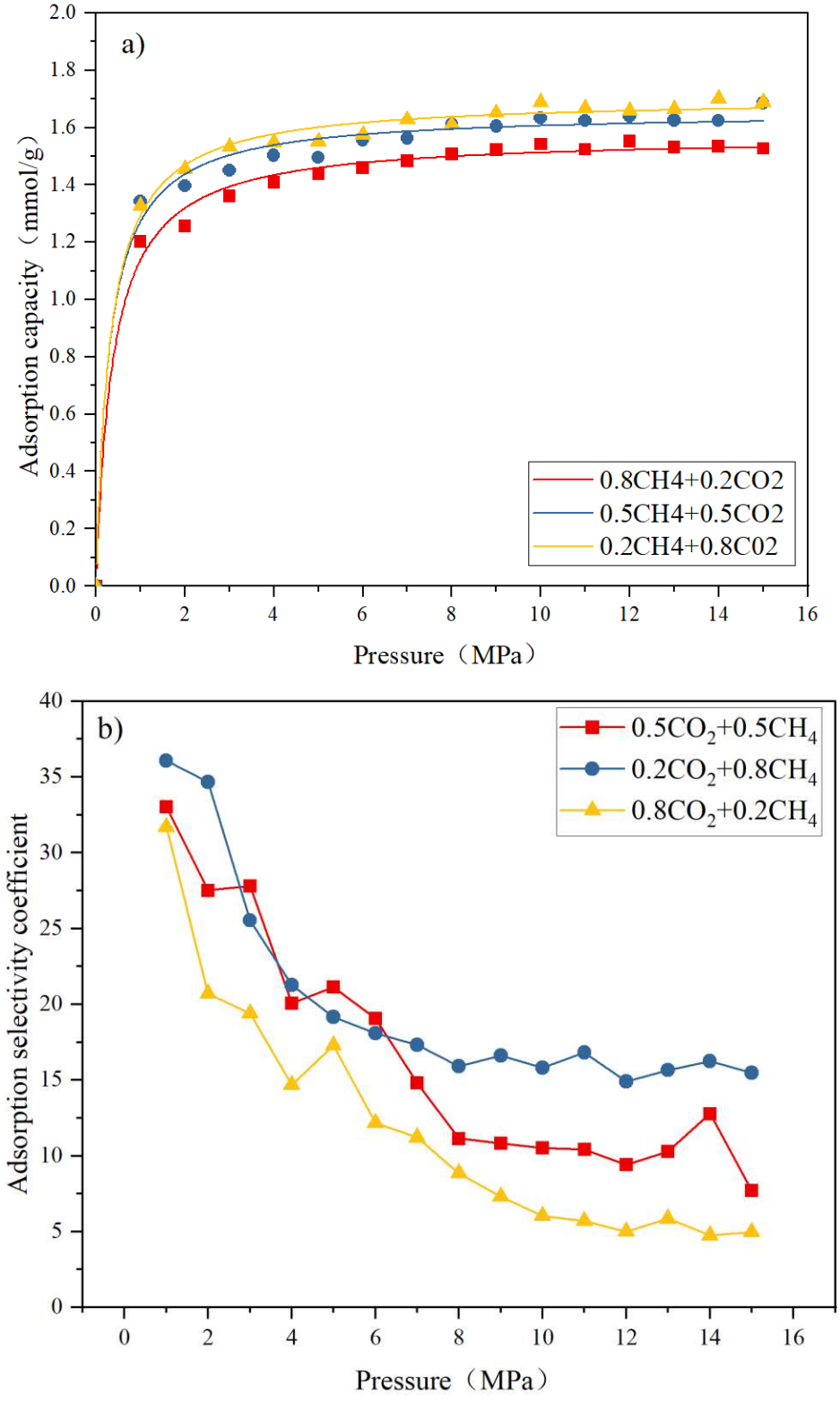

Figure 4 a)Different proportions of binary mixed competitive isothermal adsorption curves; b)Adsorption selectivity coefficients of binary mixed gases with different proportions

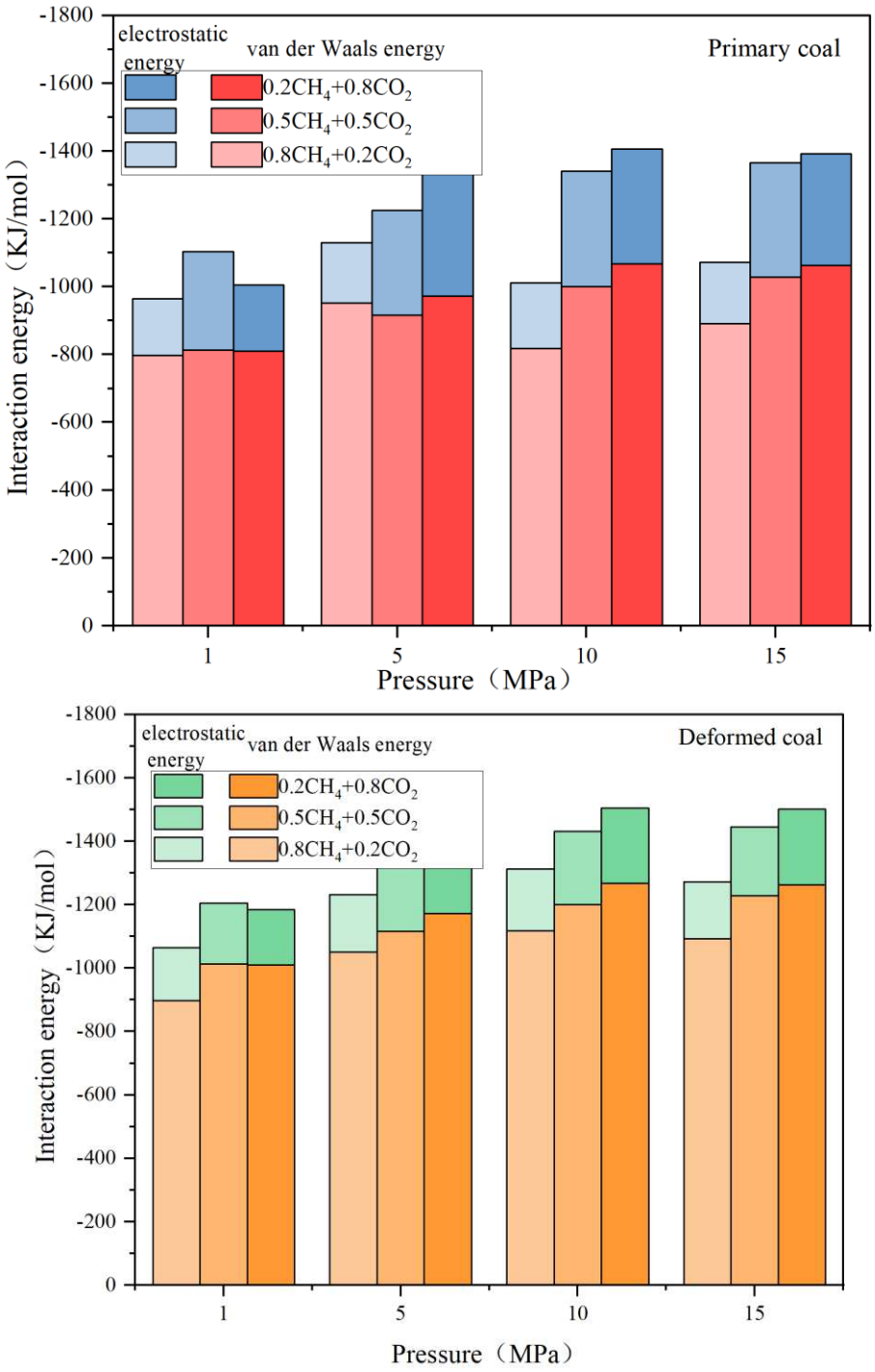

Figure 5 Interaction energy of binary mixed gases with different proportions

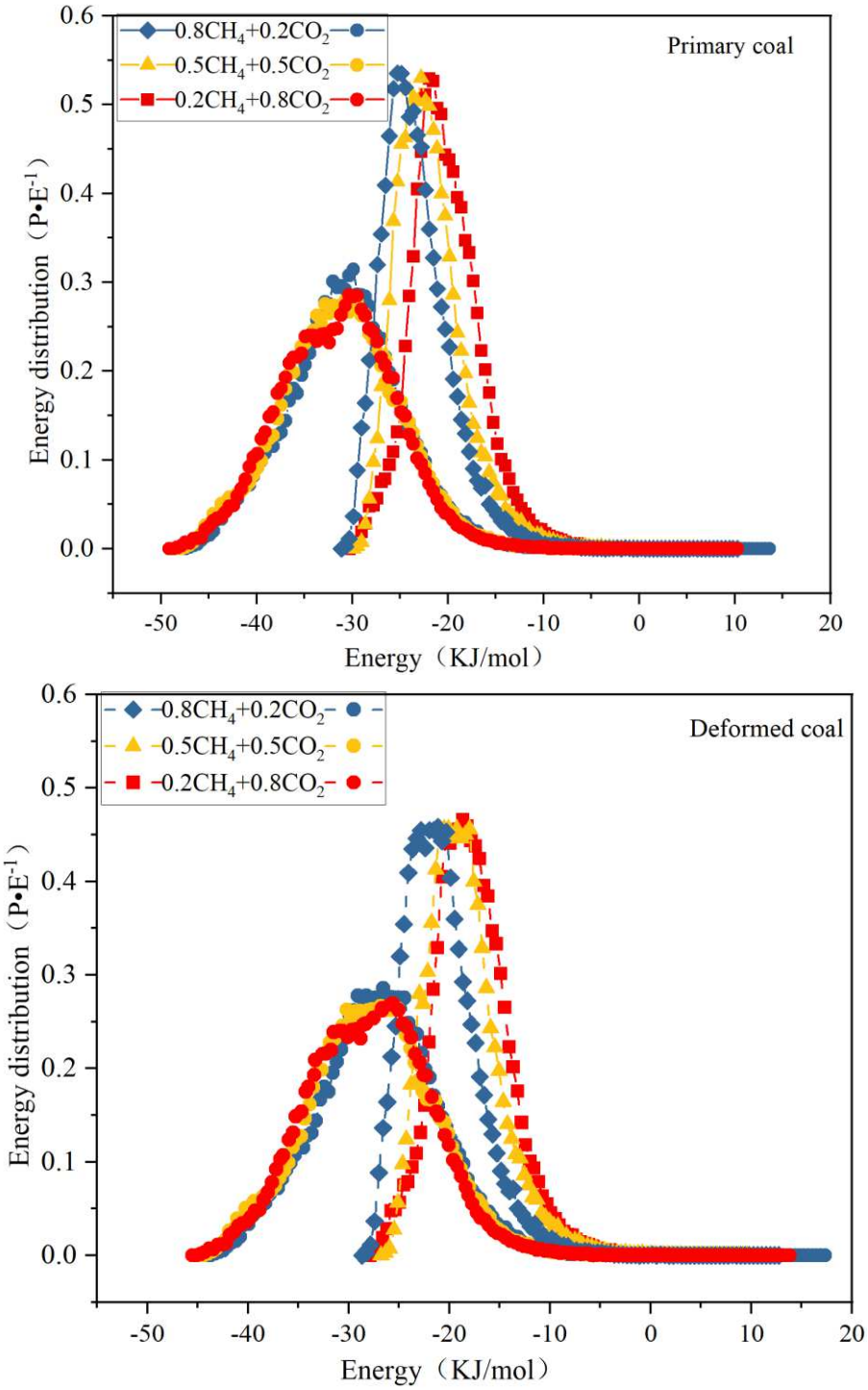

Figure 6 Adsorption energy distribution of binary mixed gases with different proportions

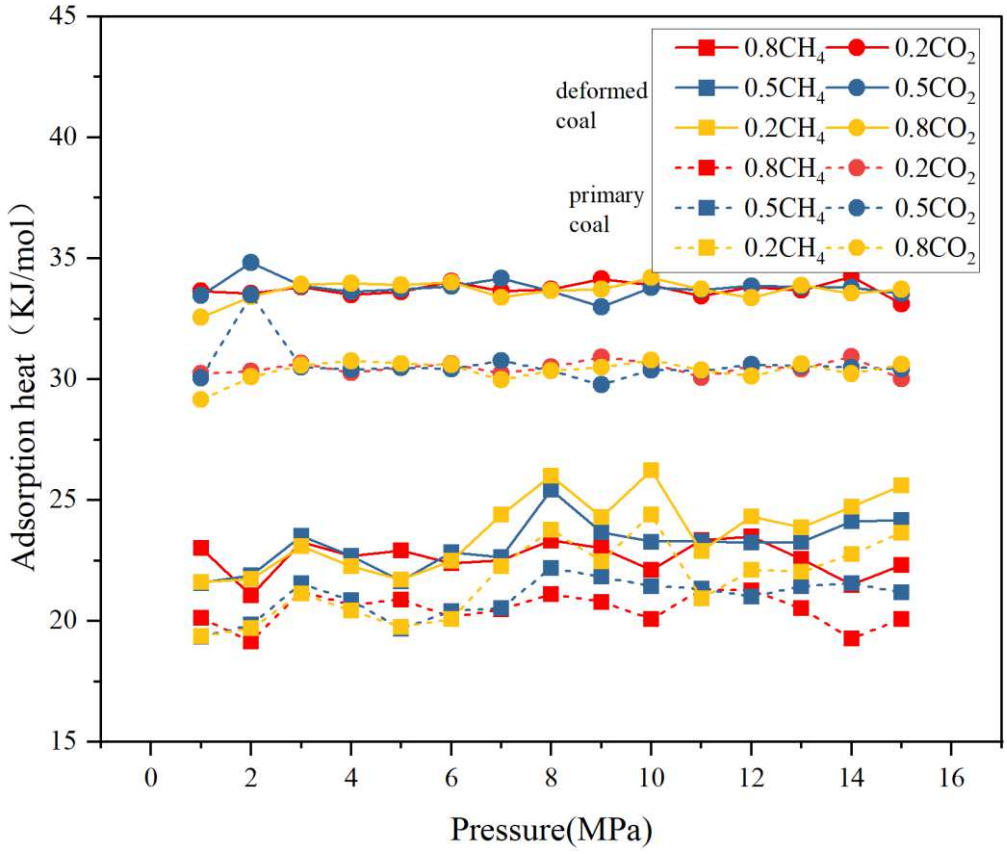

Figure 7 Adsorption heat of binary mixed gases with different proportions during adsorption

Table 1 Langmuir fitting information of isothermal adsorption data for CH4 and CO2 at different temperatures

sample	T/K	CH_4			CO_2		
		a /（mmol/g）	b /(MPa)	R^2/(%)	a /（mmol/g）	b /(MPa)	R^2/(%)
Deformed coal	283.15	1.28	0.98	96.87	1.85	14.56	76.86
	298.15	1.25	0.73	96.82	1.79	10.26	88.04
	313.15	1.18	0.59	97.78	1.72	5.65	88.03
Primary coal	283.15	1.05	0.82	95.73	1.52	11.34	75.62
	298.15	1.02	0.65	95.68	1.48	8.92	86.78
	313.15	0.98	0.51	96.54	1.41	4.88	86.55

Table 2 Langmuir fitting information of competitive isothermal adsorption curves for binary mixed gases with different proportions

sample	CH_4/CO_2	*a* /（mmol/g）	*b* /(MPa)	R^2(%)
Deformed coal	0.2/0.8	1.57	2.63	91.47
	0.5/0.5	1.65	2.91	82.76
	0.8/0.2	1.70	3.26	92.07
Primary coal	0.2/0.8	1.33	2.35	91.24
	0.5/0.5	1.40	2.62	81.53
	0.8/0.2	1.45	2.98	91.86

Table 3 Total interaction energy of binary mixed gases with different proportions

sample	P/（MPa）	Total interaction energy /(KJ/mol)		
		$0.8CH_4$:$0.2CO_2$	$0.5CH_4$:$0.5CO_2$	$0.2CH_4$:$0.8CO_2$
Deformed coal	1	-1064.79	-1204.30	-1184.40
	5	-1230.73	-1325.01	-1405.51
	10	-1312.14	-1431.50	-1505.44
	15	-1272.18	-1445.44	-1501.87
Primary coal	1	-985.62	-1102.45	-1085.32
	5	-1128.56	-1226.78	-1298.65
	10	-1205.78	-1328.94	-1396.87
	15	-1168.93	-1342.85	-1382.56